TOPICAL REVIEW

Ultrasonic neuromodulation

To cite this article: Omer Naor *et al* 2016 *J. Neural Eng.* **13** 031003

IOP Publishing Journal of Neural Engineering
J. Neural Eng. 13 (2016) 031003 (18pp) doi:10.1088/1741-2560/13/3/031003

Topical Review

Ultrasonic neuromodulation

Omer Naor[1,2,3], **Steve Krupa**[1,3] **and Shy Shoham**[1,4]

[1] Department of Biomedical Engineering, The Technion—Israel Institute of Technology Haifa 32000, Israel
[2] The Edmond and Lily Safra Center for Brain Sciences (ELSC), The Hebrew University of Jerusalem, Jerusalem 91220, Israel

E-mail: shy@technion.ac.il

Received 8 November 2015, revised 8 April 2016
Accepted for publication 11 April 2016
Published 6 May 2016

Abstract

Ultrasonic waves can be non-invasively steered and focused into mm-scale regions across the human body and brain, and their application in generating controlled artificial modulation of neuronal activity could therefore potentially have profound implications for neural science and engineering. Ultrasonic neuro-modulation phenomena were experimentally observed and studied for nearly a century, with recent discoveries on direct neural excitation and suppression sparking a new wave of investigations in models ranging from rodents to humans. In this paper we review the physics, engineering and scientific aspects of ultrasonic fields, their control in both space and time, and their effect on neuronal activity, including a survey of both the field's foundational history and of recent findings. We describe key constraints encountered in this field, as well as key engineering systems developed to surmount them. In closing, the state of the art is discussed, with an emphasis on emerging research and clinical directions.

Keywords: ultrasound, neuromodulation, brain, non-invasive

(Some figures may appear in colour only in the online journal)

Introduction

Technologies for controlled artificial modulation of neuronal activity are widely recognized as centrally important tools for both neuroscientific research and neural engineering applications. Multiple groundbreaking technologies have joined this toolbox over the past three decades, including non-invasive approaches like transcranial magnetic stimulation (TMS) and transcranial electric stimulation (tDCS and tACS) as well as inherently invasive strategies such as optogenetic and infrared neural stimulation. Each of these emerging methods has its unique strengths and applications, but also has its drawbacks and limitations. Interestingly, the attractive combination of non-invasive, reversible neuromodulation with spatial selectivity on the order of millimeters is only found currently in a lesser-known and applied technique, based on ultrasonic (US) waves. This dissonance is even more surprising, given that US modulation of neuronal activity was experimentally observed already nearly a century ago (Harvey 1929), and has been the subject of investigation since the 1950s. In contrast to diagnostic imaging and therapeutic applications of US, which have found major clinical utility, US neuromodulation was pursued by only a small number of relatively scattered academic researchers. However, in contradistinction to this protracted beginning, substantial recent technological and scientific advancements enhance this technology and now set the stage for major contributions to both clinical and scientific applications.

In particular, the recent finding that relatively low-intensity US waves can rapidly excite neurons to elicit action potentials (Tyler *et al* 2008, Muratore *et al* 2009) has sparked a new wave of investigational work in this area. In the last few years, new studies and investigators have observed both excitation and suppression of central nervous system neurons in response to multiple combinations of US parameters, experimental models and conditions. This surge of new work has dramatically increased our *empirical* knowledge-base on how to elicit such effects across model systems from rodents to humans (Tufail *et al* 2010, Legon *et al* 2014) and

[3] Naor and Krupa contributed equally to this work.
[4] Author to whom any correspondence should be addressed.

potentially provides the foundational evidence for a predictive *theoretical* understanding (Plaksin *et al* 2014). The impact of this work is particularly encouraging when weighing in the major technological breakthroughs achieved in the development of methods for accurate focusing of US waves through the skull, down to mm-sized target volumes inside the brain (Hynynen and Jolesz 1998, White *et al* 2005). These capabilities, originally pursued and applied for high-intensity focused US (HIFU) brain surgery (in which the US is used to irreversibly ablate pathological tissue), and which are also extensively investigated in the 'milder' context of blood–brain barrier (BBB) disruption for improved drug delivery to the brain (Konofagou *et al* 2012, Aryal *et al* 2014, McDannold *et al* 2015), could provide the potential for low-intensity, reversible modulation of activity in specific neural structures virtually anywhere in the human brain.

In this paper we review the physics, engineering and scientific aspects of US fields, their control and the effect they have on neuronal activity. Recognizing that secondary, long-scale modulation of hormone levels and neurotrophic factors fall outside the current paper's scope, we concentrate on 'realtime' low-intensity and reversible neuromodulation on the sub-second time scale. In the next section we provide a primer on US waves, their propagation characteristics and commonly used measures. The following sections describe major experimental findings on US neuromodulation–both foundational and recent, and then key engineering aspects and constraints of relevant systems. In closing, the state of the art is discussed, providing an outlook towards emerging research and clinical directions.

Primer on relevant ultrasonics

US wave propagation and intensity

US waves are acoustic waves caused by mechanical vibrations occurring at frequencies above 20 KHz, too high for the human ear to sense. A volume exposed to US experiences periods of nanometer scale vibrations as the wave propagates through it with velocity c. In liquid media (such as idealized soft tissues) only a longitudinal propagation mode exists, i.e. the particles are only displaced along the propagation axis of the acoustic wave. In solid hard tissue, such as the skull and skeletal bones, the acoustic disturbance can propagate in several different modes: longitudinal waves, shear waves and the weaker Rayleigh waves on the medium boundaries and Lamb waves in a thin surface. The US field is fundamentally characterized by the time-varying *pressure* and *particle velocity* u (not to be confused with wave velocity c). Sufficiently distant from a monochromatic acoustic source, the pressure takes the form of a time-harmonic plane wave, $p(r, t) = A_0 \cos(2\pi f_0 t - k \cdot R)$ where f_0 is the fundamental frequency, k is the wave vector, and R denotes location. The pressure and particle velocities are related in the linearized regime through Euler's equation:

$$-\nabla p = \rho \partial u / \partial t, \tag{1}$$

where ρ is the medium density. An important quantity of the field is the *intensity* defined as:

$$I(t) = p(t)u(t) \tag{2}$$

with units of power per area; the intensity of multiple harmonic sources $I(\omega) = \sum \frac{1}{2}\mathrm{Re}\{p(\omega)u(\omega)\}$ is the sum of their individual contributions. Time-averaged intensity $I = \langle p^* u \rangle$ is most commonly used for time-periodic or steady state fields: see figure 1 for an explanation of the commonly used averaging windows.

The intensity of an US beam propagating from a transducer attenuates exponentially with the propagation distance due to both absorption and scattering processes (dispersion is typically negligible in biological tissue), characterized by the coefficients μ_a and μ_s respectively:

$$I(x, f) = I_0(f) \exp\{-[\mu_a(f) + \mu_s(f)]x\}, \tag{3}$$

where $I_0(f)$ is the frequency-specific intensity at $x = 0$. The frequency dependence of the scattering coefficient is related to the scatterer size, shifting as it increases from an f^4 power law for microscopic scatterers to negligible dependence when their scale matches the wavelength (Morse and Ingard 1987). While in soft tissues the contribution of scattering to attenuation is roughly ~10%–15% (Bamber 1998), in bones, and especially cancellous bone, the medium heterogeneity leads to significant scattering, both attenuating and causing wavefront aberration. The absorption mechanisms are not fully understood and their frequency-dependence in bodily tissues is empirically described as a power law $\mu_a(f) = af^b$ where a and b, are parameters of the tissue that take positive values only. For wide-band signals these combined effects result in a change in the frequency content (and in the temporal pulse shape) during propagation, as the higher frequency components are more rapidly attenuated. The absorption related heating is the mechanism behind the thermal therapeutic effects of US, used in ablative surgery and possibly in the milder physical therapy, yet when targeting deep structures, the heating in more superficial tissue may be prohibitive. This is especially true in the case of the brain, where the skull also has a much higher absorption coefficient than the soft tissue (see section on transcranial US focusing).

Acoustic boundary phenomena

At the boundary between two media several phenomena may occur, depending on the media properties and the angle of incidence. For a liquid–liquid interface, the wave will undergo reflection and refracted transmission according to Snell's law, while for a liquid–solid or solid–solid boundaries mode conversions may occur and longitudinal waves will be converted to slower shear waves. In order to calculate the pressures of the transmitted and reflected waves, it can be helpful to use the acoustic impedance (a term analogous to electrical impedance)

$$Z = p/u \tag{4}$$

which can be complex, incorporating a phase angle between the pressure and velocity, and is measured in units of Rayleigh, $1\,\mathrm{Rayl} = 1\,\mathrm{Kg}\,(\mathrm{m}^{-2}\,\mathrm{s}^{-1})$. The fractions of the

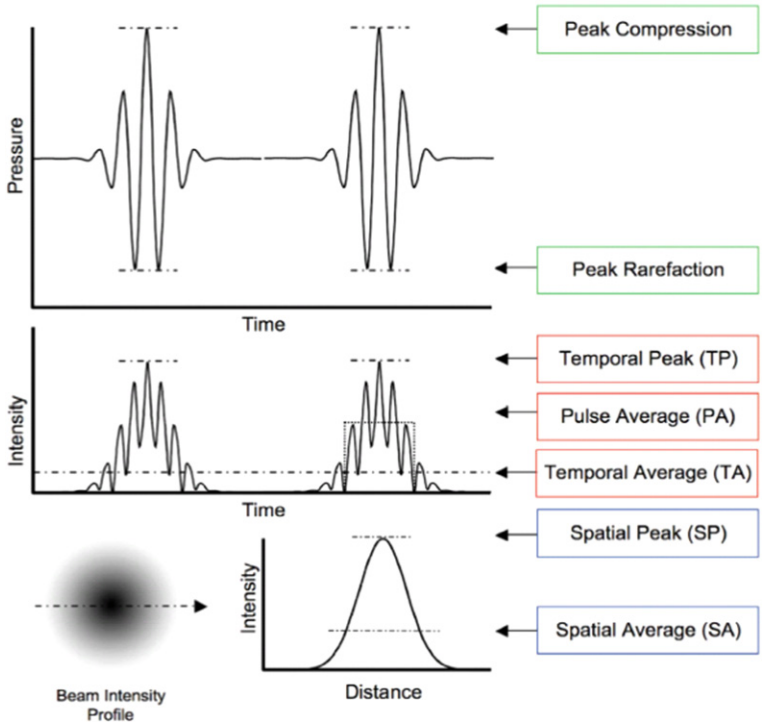

Figure 1. Visual explanation of averaging methods used to describe US pressure and intensity metrics Credit: Nelson *et al* (2009). Copyright AIUM 2009.

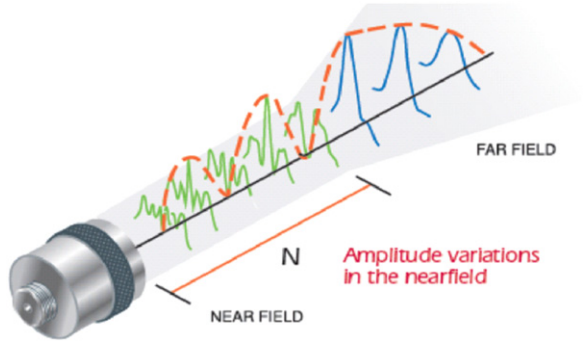

Figure 2. Visual depiction of near field to far field for un-focused ultrasound transducer Credit: 'Ultrasonic Transducers Technical Notes', reproduced with permission from Olympus (http://olympus-ims.com/en/pdf-library/).

reflectance and transmittance factors are then given by:

$$R_p = \frac{Z_2 \cos\theta_i - Z_1 \cos\theta_t}{Z_2 \cos\theta_i + Z_1 \cos\theta_t} \xrightarrow{\theta_i \to 0} R_{p\perp} = \frac{Z_2 - Z_1}{Z_2 + Z_1},$$
$$T_p = \frac{2Z_2 \cos\theta_i}{Z_2 \cos\theta_i + Z_1 \cos\theta_t} \xrightarrow{\theta_i \to 0} T_{p\perp} = \frac{2Z_2}{Z_2 + Z_1}, \quad (5)$$

where the expressions on the right side are given for the simple case of normal incidence. The fraction of energy that is reflected is given by R_p^2 and the fraction transmitted by $(Z_1/Z_2)T_p^2$.

The acoustic impedance depends on the spatial form of the wave front; for the important case of plane waves, as well as spherical waves at a distance from the source, it is simply calculated by the product:

$$Z_0 = \rho_0 c. \quad (6)$$

This relation is called *characteristic acoustic impedance* and is the impedance most often found in the literature and used for practical calculations. For example, the characteristic impedance of air is ~430 Rayl and the impedance of soft tissues is similar to that of water, i.e. ~1.5 MRayl, explaining why it is practically impossible to transmit from the air into the body. US transducers, usually manufactured from piezoelectric ceramic crystals, have much higher impedances than soft tissues and the poor *acoustic coupling* between the two media is commonly improved by introducing one or several *matching layers*, the simplest scheme being a single layer with impedance equal to the geometric mean of the input and output layers $Z_{\text{matching}} = \sqrt{Z_1 Z_2}$. Coupling ultrasound gel with impedance similar to the tissue impedance is very frequently used in medical applications, helping to mitigate the impedance mismatch caused by pockets of air trapped between the transducer and the body. The characteristic acoustic impedance is also useful for converting between intensity and pressure values for (propagating) plane acoustic waves $I = p^2/2Z_0$.

In addition to the oscillatory pressure fluctuations associated with the passage of ultrasonic pulse trains, tissue regions characterized by an abrupt change in acoustic impedance or a large increase in absorption coefficient can also experience a steady-state stress component, acting at the discontinuity boundary first exposed to the advancing ultrasonic wavefront. First measured by Altberg (1903), this

acoustic 'radiation force' arises from changes in the energy density of the acoustic field, driven by nonlinear changes in the ultrasonic properties of the underlying media (Torr 1984, Lee and Wang 1993). In subjects sonicated by focused ultrasound transducers, the heterogenous tissue oscillations associated with sharp differences in material properties (i.e. acoustic boundaries) can be measured, giving rise to several types of imaging modalities. In its general form, the acoustic radiation 'pressure' is a tensor quantity representing the acoustic radiation *stress* (Lee and Wang 1993). For a collimated ultrasonic beam impinging normally on a surface, the net acoustic radiation force F is the product of three components:

$$F = d_{\mathrm{r}} S \langle E \rangle. \tag{7}$$

(Fatemi and Greenleaf 1998) where d_{r} is the complex drag coefficient due to radiation pressure (Westervelt 1951), S is the projected surface region of the object and $\langle E \rangle$ is the time average energy density of the incident wave. The acoustic radiation pressure Γ is dependent on both the intensity I and the acoustic wave velocity $\mathbf{c}$, and can often be approximated by one of these two canonical expressions: $\Gamma = I/c$ (perfectly absorbing target), or $\Gamma = 2I/c$ (perfect reflector). For real body tissues with representative absorption coefficients, the radiation pressure associated with the ultrasonic beam is several orders of magnitude lower than the acoustic pressure of the incident beam.

A significant, potentially destructive nonlinear phenomenon associated with acoustic pressure waves in gas-soluble liquids is cavitation: the formation of tiny bubbles of dissolved gases when the media is subjected to sufficiently large negative pressures. These typically micron-scale bubbles usually aggregate around small particulate elements circulating within the fluid ('cavitation nuclei'). Cavitation can transform a homogenous fluid media into a bi-phasic mixture of gas bubble regions surrounded by liquid, creating a very complex scattering environment for acoustic pressure waves. Bubbles exposed to sufficiently high external pressures can violently collapse, generating extremely high internal pressures and temperatures, often peaking at hundreds of atmospheres and thousands of degrees Kelvin; aggressive bubble collapse within the body can result in immediate tissue destruction or future cell death via mechanical or molecular damage to key cellular components. Bubble formation in tissues is roughly dependent on the peak magnitude of the negative pressure and inversely proportional to the acoustic frequency: regulatory agencies have adopted a metric known as the mechanical index (MI) to estimate cavitation risk during ultrasound exposure

$$\mathrm{MI} = \max\{p_{\mathrm{negative}}(\mathrm{MPa}) \big/ \sqrt{f(\mathrm{MHz})}\}. \tag{8}$$

It is worth noting that the MI metric was developed assuming short (i.e. a few cycles) pulses and low duty cycles (<1%, Azhari 2010), and the max{} in equation (8) refers to the pulse's peak negative pressure.

US focusing and resolution

As in optics, propagating US waves can be focused to a confined, high intensity volume. Acoustic lenses are designed along similar principles to those of optic lenses and their resolution in the lateral (in-plane) dimension is approximately given by:

$$D_{xy} \approx \lambda F_{\#}, \tag{9}$$

where D_{xy} is the diameter of the lateral −3 dB contour and the $F_{\#}$ denotes the ratio between the distance from the array to the focal plane and the effective aperture (the lens diameter for a spherical lens). In therapeutic applications and neuromodulation research, typical US wavelengths range from 0.5 to 15 mm in soft tissue (f ranges from 0.1 to 3 MHz). The axial (z) focal dimension is usually larger by an order of magnitude. Other focusing approaches are also commonly used: geometrically designing the transducer itself to act as a lens, or employing a phased array of transducers with individually addressable elements. By driving a phased array with a spherical wave phase offset, a converging wave is generated, approximating the effect of a spherical single-element transducer. In different applications, different designs of the array and the transmission pattern are used to optimize the properties of the obtained focus, to dynamically steer the beam and to minimize undesirable phenomena, such as side-lobes outside the desired main beam (Azhari 2010).

The widely used terms near- and far-field relate to the distance from the transducer and have importance in practical ultrasonic applications. In the region near an unfocused transducer the field is highly irregular, due to the complex interference pattern dictated by diffraction, and exhibits many extremal points and large spatial gradients in all directions. The gaps between extremal points increase with the distance from the transducer, until the 'last' maxima along the acoustic (z)-axis marks the transition to the far-field, which is regular and features a well-predicted beam divergence and intensity decay. Please see figure 2 for a graphical depiction of these features. The location of this last maxima is also known as the 'natural' focus of a flat transducer (or planar array operated with all elements driven by a common source). For a circular, planar transducer, this occurs at the near-field distance $N = D^2/4\lambda$ where D is the transducer's diameter. It is usually desirable to place a target in the far-field, where the field is regular and predictable, yet proximal to the near-field distance where the intensity is maximal. The field of a focused transducer will behave similarly, yet reach the transition (and focal) point more rapidly along the z-axis. Owing to differences in the acoustic field on either side of the near-field distance N (or focal point), the −3 dB focal contour in the axial direction is typically asymmetric, with the focal point falling closer to the near-field portion of the (axial) acoustic field profile.

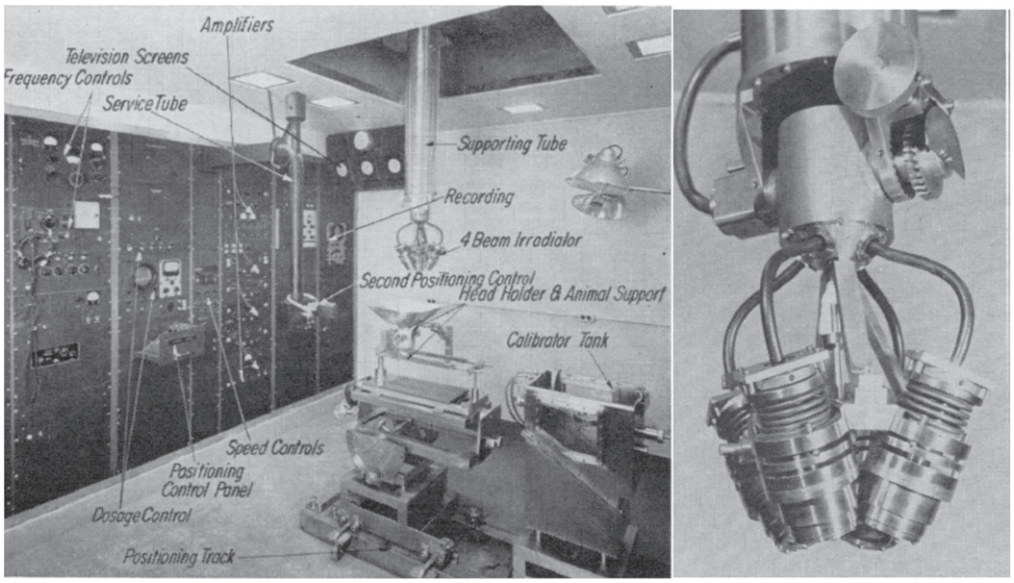

Figure 3. Experimental US sonication apparatus used by the Fry brothers *et al* in the 1950's Credit: W J and F J Fry 1960 Fundamental neurological research and human neurosurgery using intense ultrasound *IRE Trans. Med. Electron*. Copyright IEEE 1960.

Ultrasonic neuromodulation results

Foundational history

The first demonstration of ultrasonic effects on excitable tissue dates back to the 1920s (Harvey 1929) where 'subminimal twitching of the gastrocnemius muscle' were observed upon US irradiation of the frog's sciatic nerve, together with a more prominent effect on the beating heart. Later groundbreaking work by the Fry brothers and colleagues in the 1950s (Jagannathan *et al* 2009), explored advanced ultrasonic instrumentation and applications, among which they demonstrated reversible modulation of visual evoked potentials (VEPs) in cats (Fry *et al* 1958). For an example of the equipment used in this era, please see figure 3. Between these very early pioneering studies and the beginning of the 21st century, a considerable number of studies examined US effects on peripheral receptors, nerves and on brain excitability (extensively reviewed in Bystritsky *et al* 2011, Gavrilov and Tsirulnikov 2012, Gavrilov 2014), with much of this work being done in the 1970s and 1980s in the Soviet Union, by Gavrilov, Vykhodtseva and their colleagues. In this section we highlight prominent aspects of US neuro-modulation in this body of literature.

One major research thrust during this period investigated the possibility of using ultrasound to stimulate peripheral mechanical receptors underneath the skin and in the auditory system of both animals and humans (Gavrilov *et al* 1977a, 1977b, 1996). Human hands were irradiated for 1–100 milliseconds with 0.48–2.67 MHz continuous wave (CW) US stimuli, and as the intensity increased, tactile, heat and pain perceptions were reported in this order and in a strongly frequency dependent manner (e.g. pain sensation threshold of 55 W cm^{-2} at 0.48 MHz and 2860 W cm^{-2} at 1.95 MHz). Interestingly, the investigators reported that the threshold displacement amplitude at the focal region was independent of frequency, suggesting a mechanical rather than thermal mechanism, a notion further supported by the fact that sensations at low frequencies occurred with a temperature increase of less than 0.1 °C. A study of the frog Pacinian corpuscle showed that short (0.1–1 ms), low intensity (0.4–2.5 W cm^{-2}) US stimuli directly evoked receptor potentials (Gavrilov *et al* 1977b).

Responses in the frog auditory midbrain area were elicited with 0.48 MHz US waves (1–100 ms, 0.01–1 W cm^{-2}, Gavrilov *et al* 1977b), and cochlear and auditory nerve potentials were elicited in cats with US waves directly transmitted through their temporal lobe dura mater (Foster and Wiederhold 1978). Later, amplitude modulated (AM) waves with an US carrier frequency but auditory-range modulation frequencies, were directed at the human cochlea and invoked hearing sensations (Tsirulnikov *et al* 1988). While it seems intuitive to suggest that radiation forces at the audible modulating frequencies are responsible for these effects, a detailed discussion of this and alternative mechanisms is found in Gavrilov and Tsirulnikov (2012).

A second group of studies was concerned with large scale ultrasonic modulation of brain excitability. In Koroleva *et al* (1986), repetitive 50–100 ms US pulses were directed to the cortex, thalamus, hippocampus, and caudate nucleus of rats. The US pulses were reported to cause a steady negative potential shift of several mV, often leading to waves of spreading depression with amplitudes of 20–30 mV, and occasionally followed by convulsive discharges. In Velling and Shklyaruk (1988) the temporal, sensorimotor, and parietal cortex of cats and rabbits were targeted with low intensity (1–100 mW cm^{-2}) focused US (FUS) pulses, leading to increase or decrease of the electrocorticogram (ECoG) rhythm amplitude, depending on the intensity and modulation frequency (lower intensities and frequencies led to increased amplitude). FUS also modulated the amplitude of light-

evoked potentials and thresholds for electro-stimulation in the motor cortex, in a similar intensity dependent manner (Velling and Shklyaruk 1988). For a comparison of the brain sonication parameters used by researchers during this era as well as in more recent studies of related CNS-neuromodulatory effects of extended ultrasound exposure, see table 1.

A third and final theme examined ultrasonic effects on peripheral and central nerve *fibers* (Takagi *et al* 1960, Young and Henneman 1961, Lele 1963, Mihran *et al* 1990, Rinaldi *et al* 1991, Bachtold *et al* 1998). Most of these studies involved medium to high US intensities (10–100 s of $W\,cm^{-2}$) at US frequencies from 0.5 to 3 MHz (typical to therapeutic US applications), and reported impaired conduction after sonication, although elevated compound action potential (CAP) amplitudes and reduced latencies were also found for specific US parameters (Takagi *et al* 1960, Lele 1963, Mihran *et al* 1990). In most experiments long irradiation durations (several seconds to minutes) were used, with the notable exception of a study in which single, 0.5 ms bursts of 50–750 $W\,cm^{-2}$ were shown to cause enhancement and suppression of the CAP (Mihran *et al* 1990). In some cases, the researchers also applied global thermal stimuli without the presence of US waves in an attempt to find out whether the effects of the US stimuli are entirely based on the thermal changes they introduce to the tissue. According to Lele (1963), this was the case, while in Takagi *et al* (1960) only the suppressive effects were replicated by thermal stimuli and in Mihran *et al* (1990) radiation force, mechanical rather than thermal in nature, was suggested as the underlying bio-physical mechanism. Two related recent studies found reductions in CAP amplitude in frog sciatic nerves (Colucci *et al* 2009) and rat vagal nerves (Juan *et al* 2014) coupled to moderate increases in temperature within the target regions when using US durations and intensities in a generally similar range to the earlier studies (>10 s, $\gg 10\,W\,cm^{-2}$). In (Juan *et al* 2014), a decrease in the nerves' conduction velocity was also reported.

Recent findings

This section provides a summary of key findings published since the turn of the millennium, including first demonstrations of neural stimulation in the mammalian CNS, inhibitory and excitatory regimes, characterization of the effects of stimulus intensity and duration on the response latency and strength, anesthesia, and other relevant parameters. For a tabulated summary of the US pulse-train parameters used in these recent studies, see table 2.

Brain

Small animal studies

Two pioneering studies presented in 2008 reported a novel type of interaction between neurons and ultrasound, and inspired additional experiments which aimed to cause direct and localized neuronal excitation in the CNS. In their 2008 conference paper, Muratore and colleagues showed that short, low intensity US pulses (100 μs, up to 77 kPa of 4.04 MHz US) cause neurons in mouse hippocampal slice cultures to generate action potentials (Muratore *et al* 2009). Then, in their landmark study, Tyler and colleagues applied low power, 0.44–0.67 MHz US to hippocampal slice cultures and *ex vivo* brains of mice in several transmission parameters (Tyler *et al* 2008). Their results included observation of time-locked action potentials, rises in intracellular Ca^{2+} and Na^{+} that were only partially abolished by tetrodotoxin (TTX) and Cd^{2+}, and indications for synaptic vesicle release.

These *in vitro* studies were followed by a group of *in vivo* studies in anesthetized rodent and rabbit models, examining the excitatory and inhibitory effects of US stimuli on different brain areas, as observed by induced muscle activity, evoked potentials, microelectrode recordings and fMRI (Tufail *et al* 2010, Min *et al* 2011a, Yoo *et al* 2011a, Yang *et al* 2012, King *et al* 2013, Younan *et al* 2013, Mehic *et al* 2014, Kim *et al* 2014a, 2015). Motor responses were elicited in mice (Tufail *et al* 2010, King *et al* 2013, 2014, Mehic *et al* 2014, Kamimura *et al* 2015), rabbits (Yoo *et al* 2011a) and rats (Younan *et al* 2013, Kim *et al* 2014a, 2014b), in response to pulsed-wave (PW) and CW US stimuli directed to somatomotor cortical areas. Exploring the stimulation parameter space, these studies consistently suggest that the stimulus durations necessary for eliciting a response were on the order of *tens to hundreds of milliseconds* of high duty cycle US stimulation and that low frequencies are indicated as preferable to higher ones (250–350 KHz versus 500–650 KHz) (Tufail *et al* 2010, King *et al* 2013, Kim *et al* 2014a). Put together, the accumulating data suggests an overall positive relation between the stimulus' intensity, duration and duty cycle and the response strength and likelihood (King *et al* 2013), although it is quite plausible that an optimum 'sweet spot' exists for some high parameter values (e.g., 50% duty cycle and 300 ms stimuli), above which the response decreases (Kim *et al* 2014a). Importantly, anesthesia levels were indicated in these studies to play a major role in the neuronal susceptibility to US stimuli: only light levels of anesthesia were found to be suitable for eliciting neuronal responses (King *et al* 2013, Kim *et al* 2014a), which were abolished upon increase in the anesthetic dose (King *et al* 2013).

The suppression of evoked electroencephalography (EEG) potentials, already described by Fry *et al* (1958) who transmitted CW stimulation to the cat lateral geniculate nucleus (LGN), was observed upon low, 5% duty cycles, cortical sonication in rabbits (Yoo *et al* 2011a) and rats (Kim *et al* 2015). Besides the anticipated result that a time-averaged intensity (I_{TA}) threshold must be exceeded to significantly attenuate the response, an intriguing finding was that further increasing the intensity or the duty cycle by 66% reversed the effect and led to significant and prolonged facilitation of the evoked response (Kim *et al* 2015). Non-cortical areas in which the effect of US were studied were the hippocampus, where extracellular spikes and local field potentials were measured in response to US stimuli (Tufail *et al* 2010), and the thalamus, wherein PW bursts of 650–690 KHz US

Table 1. Summary of *in situ* pulse parameters for *in vivo* US neuromodulation, foundational history.

US target (Researcher)	Modulation effect	Frequency (MHz)	I_{sppa} (W cm^{-2})	T_{US_Stim} (s)	PRF (Hz)	Duty cycle %
Cat: LGN (Fry *et al* 1958)	Partial VEP suppression	0.98	1.35	20–120		100
Cat: edinger/wesrpal nucleus (Ballantine *et al* 1960)	Functional response of eye pupil	2.7	1700[a]	0.14	0.33	4.6
Cat: spinal cord	Reflex enhancement (reversible)		350[a]	3	0.33–1	10–30
	Reflex depression (post- sonication)		350[a]	51–555	0.33	10
Cat: optic tract/LGN (Adrianov *et al* 1984)	VEP suppression	0.98	7–63[b]	10–60	0.5–50	30–60
Rat: cerebral cortex (Koroleva *et al* 1986, Vykhodtseva and Koroleva 2006)	Change in DC potentials	4.6	236	25		100
Rat: hippocampus	DC change, spreading depression (SD) induction		79	25	5	50
Rat: thalamus	DC change, SD induction		79	25	5,10	25, 50
Rat: caudate nucleus	DC change, SD induction		157, 79	15, 25	5	50
Rat: cortex (Vykhodtseva and Konopatskaya 2007)	ECoG suppression	4.89	1.8 W[c]	25–40	2	2–40
Rat: thalamus (Yoo *et al* 2011b)	Early waking from anesthesia	0.65	6	1200	100	5
Rat: thalamus (Min *et al* 2011a)	Seizure suppression	0.69	2.6	180	100	5
Rat: thalamus (Min *et al* 2011b, Yang *et al* 2012)	increases in dopamine, serotonin (2011b) and decrease in GABA (2012)	0.65	3.5	1200	100	5
Human: posterior frontal cortex (Hameroff *et al* 2013)	Improvements in mood, modest pain reduction	8	0.15[d]	15	527_{max}	0.01

$\mathbf{T}_{US\_Stim}$ = stimulus duration of applied US.
[a] I_{sppa} or I_{sptp}.
[b] I_{sapa} (focus).
[c] 1.8 W $\sum$ acoustic power.
[d] I_{spta}.

Table 2. Summary of *in situ* pulse parameters for recent studies on US neuromodulation of CNS circuits.

US target (Researcher)	Modulation effect	Frequency (MHz)	I_{sppa} (W cm^{-2})	T_{US_Stim} (ms)	PRF (Hz)	Duty cycle %
In vitro: rat hippocampal slice culture (Muratore 2009)	US-evoked electrical responses from cell culture, recorded using MEA	4.04	0.19	0.1		100
In vitro: mouse hippocampal slice culture (Tyler *et al* 2008)	Na^+ and Ca^{2+} transients in CA1 neurons	0.44 and 0.67	2.9 and unstated	5 s and 373	0–100 and 10	<0.23 and 74.5
In vitro: mouse isolated brain	Ca^{2+} transients on dorsal surface	0.44	2.9	5 s	0–100	<0.23
Mouse: motor cortex (Tufail *et al* 2010)	Visible muscle twitches, increases in LFPs, M1 MUAs, EMG	0.25–0.5	0.08–0.23	26–333	1200–3000	19–86
Mouse: hippocampus CA1	Increases in LFPs @0.25 MHz, BDNF production @0.35 MHz	0.25 and 0.35	0.26 and 0.17	~330	2000 and 1500	32 and 21.4
Mouse: motor cortex (King *et al* 2013)	EMG spiking (CW, full parametric space, US duration and intensity)	0.5	0.3–16.8	20–480		100
	(Frequency sweep)	0.25–0.6	0.02–16.8	40/*f*(MHz)		100
	(CW versus PW)	0.5	1–79	80	1500	30 and 100
	(PRF sweep)		4.2–30	120/PRF(kHz)	100–3000	20*PRF(kHz)
Mouse: motor cortex (King *et al* 2014)	Increased EMG spiking	0.5	3	80		100
Mouse: cerebrum (Mehic *et al* 2014)	Limb/tail/whisker movement	0.5	17.5	59	1500	30
		1.75–2.25	13–27	15–59	1500	15–30
Mouse: cerebrum and deeper nuclei (Kamimura *et al* 2015)	Paw and tail motions	1.9 MHz	66–158	1 s	1000	50
	Eye movements, pupil dilations		45–158	1 s	1000	50
Rabbit: motor cortex (Yoo *et al* 2011a)	forepaw twitches, increases in BOLD (fMRI), EMG spiking	0.69	3.3–12.6	1 s	10	50
Rabbit: visual cortex	Partial VEP suppression, BOLD (fMRI) and increase p30 of VEP		3.3–6.4	>7–8 s	100	5
Rat: abducens cranial nerve (Kim *et al* 2012)	Abduction of eyeball, ipsilateral to US site	0.35	8.6–20	200	1500	54
Rat: cerebrum (Younan *et al* 2013)	Strong tail, hind leg movement	0.32	>=7.5 (17.5[a])	250	2000	47
Rat: motor cortex (Kim *et al* 2014a)	Tail twitches	0.35, 0.65	4.9–22.4	150–400	60–2800	30–100
Rat: unilateral thalamic area (Kim *et al* 2014b)	Tail twitches, elevated glucose uptake from the PET image	0.35	6	300	1000	50
Rat: visual cortex (Kim *et al* 2015)	VEP elevation	0.35	3 and 5	150 × 1 s	166 and 100	8.3 and 5
	VEP suppression		3	150 × 1 s	100	5
Sheep: primary sensorimotor SM1 (Lee *et al* 2016)	Hind leg EMG spiking from US stimulus @SM1	0.25	3.4–11.8	300	500	50
Sheep: visual V1 areas	EEG response to US stimulation @V1, no visual stimulation applied		1.7–14.3	300	500	50
Primate: frontal eye field, pre-motor cortex (Deffieux *et al* 2013)	Delay in anti- saccade during trained visual task	0.32	2.9–5.1	100		100
Human: primary somatosensory cortex S1 (Legon *et al* 2014, Mueller *et al* 2014)	Changes in EEG, 2 point discrimination improvement	0.5	5.9[b]	500	1000	36
Human: primary somatosensory cortex S1 (Lee *et al* 2015)	Changes in EEG, limb sensations linked to S1 US target	0.25	0.3–2.5	300	500	50
Rat: retina, widefield stimulus (Naor *et al* 2012)	Ultrasound evoked potential stimulation (~25% of VEPs)	0.5	0.1–0.4	5–20	1900–2000	10–20
		1	5.2–8.5	10–20	1667	16.7
Salamander: retina, focused stimulation (Menz *et al* 2013)	Retinal stimulation	43	20–60	1 s		100

$\mathbf{T_{US\_Stim}}$ = stimulus duration of applied US.
[a] Corrected for standing waves.
[b] Estimate from skull fragment test.

directed at the thalamus of rats led to a decrease in epileptic seizures and EEG bursts (Min *et al* 2011a), and increased levels of frontal lobe GABA, dopamine and serotonin (Min *et al* 2011b, Yang *et al* 2012).

Large animals, human and non-human primates

In vivo rodent studies, albeit instrumental in the development of US neuromodulation procedures, are technically limited by (i) the formation of standing wave patterns within their small skulls (Younan *et al* 2013), and (ii) the requirement for maintaining low anesthesia levels (King *et al* 2013). These limitations, and the ultimately translational motivations of most of the research in this area have led to the rapid development of experimental applications in non-human primates and in humans. An early study with human subjects (Hameroff *et al* 2013) reported non-specific mood effects when applying low intensity high-frequency (8 MHz) US for 15 s to the scalp region overlying the frontal-temporal cortex. A series of very recent studies explored specific stimulus-locked neuromodulatory effects, beginning with the pioneering study by Aubry, Pouget and colleagues (Deffieux *et al* 2013) who applied low-intensity ultrasound to the frontal eye field (FEF) of Macaque Rhesus monkeys performing a visual task. Deffieux *et al* demonstrated that the 320 KHz US pulse led to significant, transient modulation of anti-saccade latencies in the contra-lateral visual field and to slower eye movements and postulated a FUS-induced disruption of processing across the FEF to account for the findings.

This early report of US neuromodulation in a non-human primate was rapidly followed up by reports from the Tyler and Yoo teams demonstrating the use of FUS to modulate the activity of the *human* primary somatosensory cortex (S1) (Legon *et al* 2014, Mueller *et al* 2014, Lee *et al* 2015). Legon, Mueller and their colleagues transmitted 500 KHz FUS (I_{sppa} 23.87 W cm^{-2}) towards S1 and noted amplitude reductions and spectral content changes in the somatosensory evoked potentials (SEP) and intrinsic EEG. Data from electrodes centered about the CP3 electrode site, where the US transducer interfaced with the scalp, showed that the US stimuli modulated SEPs elicited by median nerve stimulation, preferentially modulated the phase of beta wave activity in intrinsic EEG signals, and affected both beta and gamma wave activity in evoked EEG responses. Behaviorally, FUS targeted to S1 enhanced performance on sensory discrimination tasks, without influencing task attention or response bias. Notably, the changes produced by FUS on sensory-evoked brain activity were abolished upon focusing the US beam 1 cm anterior or posterior to S1 (connoting superior spatial specificity over existing noninvasive neuromodulatory modalities).

In contrast, Lee *et al* (2015) used extra-cranially applied FUS to elicit and characterize limb-specific somatosensory sensations in the absence of external sensory stimuli, and corroborate the effect of FUS on median nerve stimulation-induced SEPs. The broad spatial extent of limb sensation (in some patients) elicited by the FUS stands in contrast to a prior rat study which correlates a high localization of glucose uptake (via PET scan imaging) in the motor cortex during sonication with high spatial specificity ($\ll$FWHM) of the applied 350 kHz FUS stimulus (Ispta 0.35 W cm^{-2}, Kim *et al* 2014b).

In each of these studies, an effort was made to estimate the effect of the primate or human skull on the transmitted US waves, generally much more significant than that of the rodent skull. The total Macaque skull effect was estimated as a 42% (~4 dB) reduction in power (Deffieux *et al* 2013), while curiously, both studies on humans reported attenuation of ~6 dB, in spite of the different US frequencies (250 KHz in Lee *et al* 2015 and 500 KHz in Legon *et al* 2014). In Lee *et al* (2015) the investigators added an important technological innovation: the integration of CT and MRI skull and brain data into a full-wave, commercial acoustic simulation model, allowing detailed per-subject assessment of the US field. This combined imaging/simulation modality facilitated a better understanding of the (considerable) consequences of inter-subject variations in cranial and neural anatomy, exemplified by the correlation found between reduced acoustic intensities at the targeted S1 'hand' region (via US beam deviation) and the absence of somatosensory sensations. Importantly, primate studies do not fully replace more accessible, large brain animal models where activation mechanisms and safety can be carefully studied. Lee *et al* (2016) recently demonstrated successful neuromodulation of sheep primary sensorimotor and visual cortical targets. The researchers noted a high degree of variability in acoustic intensity activation thresholds between the animals (I_{sppa} ~ 2–11 W cm^{-2}). The correlation between the applied acoustic intensity and the magnitude of the recorded motor evoked potentials (MEPs) and VEPs also varied across the test subjects. In contrast to earlier rodent studies, the MEPs were only detected in the limb contralateral to the SM1 target site, without any detectable muscle movement.

Retinal stimulation

In an interesting parallel to its unique role as the optically accessible part of the CNS, the retina is also arguably the most easily accessible structure in the CNS to high frequency US waves, which are widely used for diagnostic imaging of the retina. This accessibility makes the retina an interesting target for studies of both basic and applied US neuromodulation.

In recent work, we proposed the use of ultrasonic stimulation of the retina as an alternative approach to vision restoration in cases of retinal degeneration (Naor *et al* 2012). In addition to an engineering investigation of the potential resolution and channel numbers, safety issues and wave shaping demonstrations, we recorded potentials from the scalps of anesthetized rats evoked by US transmitted towards their retina. Responses were found to bursts of 0.5 and 1 MHz US waves, with peak acoustic pressures ranging from 86 to 725 kPa, total durations of 5–20 ms and PRF on the order of 2 KHz. These responses were abolished or significantly decreased after TTX injection to the intravitreal space

adjacent to the retina. In the isolated salamander retina, Menz *et al* (2013) investigated responses to stimulation with high frequency, 43 MHz US. They found repeatable spike responses to both US onset and cessation, that intensity increases led to increased firing rates and decreased latencies (saturating at 10–30 W cm^{-2}), and indifference to changes in the pulse repetition rate (15 Hz–1 MHz). Most neurons responded with shorter latencies to US than to visual stimuli, and to US cessation than onset. The tight focal spot (−3 dB at 90 μm) enabled the observation of phenomena similar to the visual center-surround antagonism and differences in the US-receptive fields for stimulus ON and OFF responses, indicating that the retinal ganglion cell (RGC) spike responses are at least partially mediated by presynaptic cells. Pharmacological manipulations indicated only a minor contribution of photoreceptors in the process, and a critical role played by Ca^{2+} currents. OFF responses were also observed in RGC single-units in isolated mouse retina in response to 2.3 MHz CW US stimuli from a clinical phased array transducer (Naor, PhD Thesis).

Systems and constraints

Ultrasonic challenges of the brain and skull

Initial experiments attempting to localize ultrasonic fields within the body found a high probability of collateral tissue damage from using smaller, single element US transducers and 'open water' targeting methods. In demonstrating successful ultrasonic lesioning of *ex vivo* tissue, Lynn *et al* (1942) observed significant tissue trauma along the acoustic path formed between their spherical transducer and the intended target location, which they proposed to minimize using 'a mosaic of 4 to 6 two-inch curved crystals, all focusing on a common point'. Scientists soon explored the use of HIFU for treating brain pathologies (Fry *et al* 1954, Lindstrom 1954, Jagannathan *et al* 2009), as well as for reversible modulation of neural function (Fry *et al* 1958, Ballantine *et al* 1960). The promise of these pioneering *craniotomy-based* studies inspired future *non-invasive* research studies, identifying the main impediments to accurate targeting/lesioning within the brain. Cardinally, researchers demonstrated that the high acoustic reflectance of the human cranium significantly limits the ultrasonic frequencies used in transcranial therapeutic ultrasound (typically less than 1.3 MHz, see Fry and Barger 1978). Constraints on frequencies and pulse lengths employed are also encountered in studies involving small animals (O'Reilly *et al* 2011), where the skull thickness and composition are also a key factor for effective transcranial US targeting.

Additional insights into ultrasonic transmission through cranial bone also come from detailed numerical modeling. A recent simulation of the interaction between US and the human skull reports that thermal absorption plays a relatively minor role in the cranial attenuation of ultrasonic energy (Pinton *et al* 2012a), in contrast to long-standing concerns regarding heat production within and around the skull in response to transcranial acoustic wave propagation (Carstensen *et al* 1990, McDannold *et al* 2004). Instead, processes associated with wavefront redirection (reflection), scattering, and transformation (mode conversion) are reported to comprise the major loss mechanisms associated with the passage of ultrasonic pulse-trains through the skull (Pinton *et al* 2012a). Because small-animal cranium dimensions are comparable to the ultrasonic wavelengths employed, simulations of US pulse propagation within the rat skull highlight the existence of interference effects (standing waves) between the incident and reflected fields, leading to the generation of distorted pressure distributions (Younan *et al* 2013).

Modern HIFU hardware and computational tools

Significant advances made in transcranial US targeting motivated mainly by the prospects of non-invasive HIFU surgery, greatly improve the potential for accurate US neuromodulation in humans. The challenge of eliminating collateral tissue damage steered HIFU development efforts towards multi-element, phased array ultrasound systems, whose essential elements are (i) a structured collection of transducers oriented/aimed in the same general direction, and (ii) means to control the phase/timing (and possibly amplitude) of the radio frequency (RF) signals driving each transducer. Figure 4 provides a conceptual sketch of a phased array in action: time delays in the driving signals applied to each element allow the ultrasonic beam to be steered and focused in a variety of ways. Figure 5 shows a modern surgical HIFU array, the Insightec ExAblate 4000, capable of generating millimeter scale lesions within the brain. Figure 6 depicts the full Insightec 'ExAblate Neuro' MR-guided focused ultrasound neurosurgery system in operation. Phased arrays do not necessarily need to be organized on a regular grid: random element configurations may further reduce unintended thermal trauma (Hand *et al* 2009). Operating the HIFU array inside a non-invasive, wide-field MRI scanner allows the operator to periodically assess and modify the spatio-temporal extent of the ultrasound treatment region, indicated by localized temperature elevation or tissue displacement.

Hardware solutions based on phased arrays generally provide sufficient wavefront shaping controls and degrees of freedom to realize a wide range of possible pressure field distributions after passing through complex acoustic structures like the human skull, but require numerical simulation and beam steering algorithms to provide the array inputs needed to optimally focus the acoustic field over the desired target region(s). To address this challenge, numerical simulation/targeting solutions typically apply the reliable but computationally 'expensive' finite difference time domain (FDTD) simulation method, coded to simulate a time reversal experiment. In this approach, the extra-cranial phase distortions are computed from the outwardly propagating wavefronts launched by a virtual, in-skull ultrasonic point source (Thomas and Fink 1996, Pinton *et al* 2012b). Owing to the principle of acoustic reciprocity, these computed phase distortions are equivalent to the phase corrections needed to

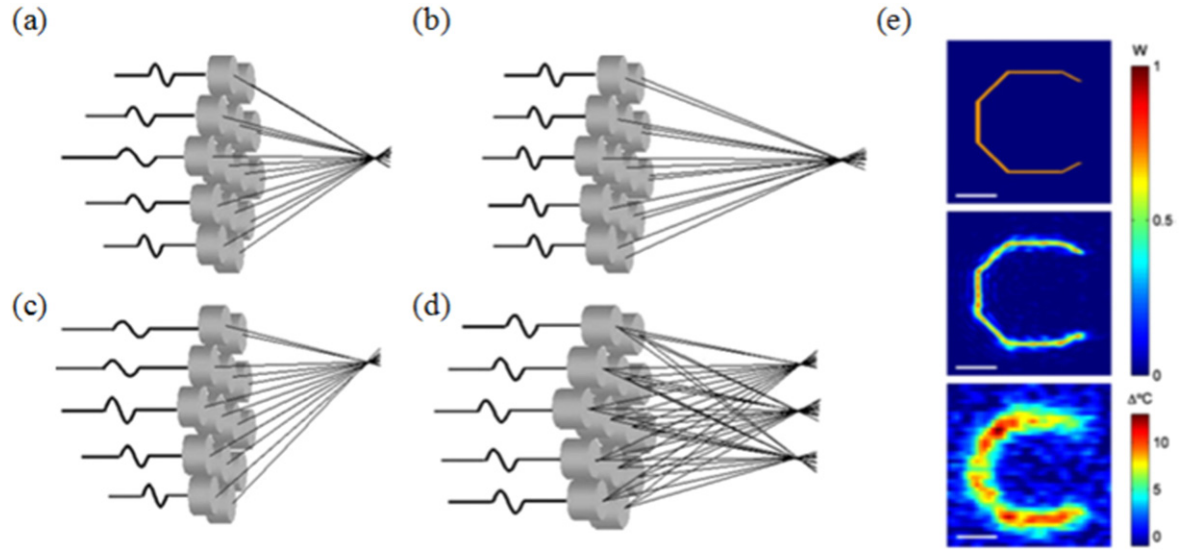

Figure 4. An ultrasound phased array has the ability to control the location of the focus by varying the phase and amplitude of the RF-signals driving each element. A singular focus can be established along the central axis of the array (a), scanned axially to a deeper region within the target tissue (b), and to an off-axis target region (c). Advanced beamforming algorithms can permit multi-focal targeting solutions (d). Panel (e) demonstrates a beamforming algorithm inspired by optical holography. A 2D input pattern (top) drives the computation of phase offsets used to control a 2.3 MHz, 987 element phased array, in both simulation (middle, acoustic intensity map), and in reality (bottom, MR-measured temperature gradients). The focal plane is 25 mm away from the array aperture, the pattern size is 15 mm. Credit: Jolesz and Hynynen (2008) (panels (a)–(d)), copyright Taylor and Francis Group LLC Books 2007. Naor *et al* (2012) (panel (e)). Copyright IOP Publishing 2012.

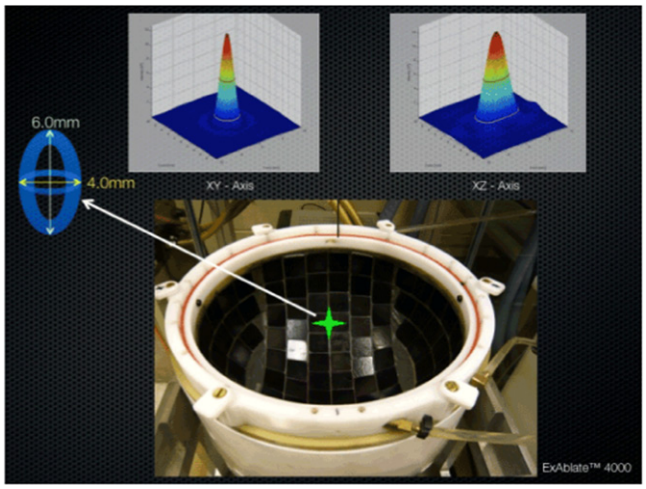

Figure 5. Top view inside the hemispheric transducer of the ExAblate™ 4000 HIFU headsystem. Each black tile contains nine single ultrasound transmitting elements (total $N = 1000$). All elements transmit towards the center of the transducer (green star), creating a sharp focus beam of 4.0 mm diameter in lateral and 6.0 mm in elevational orientation. Parametric images of the focus, based on acoustic measurements, are given in *XY* (upper left)—and *Z* (upper right)—orientation. Credit: Hölscher *et al* 2011 Noninvasive transcranial clot lysis using high intensity focused ultrasound *J. Neurol Neurophysiol*. Copyright OMICS International 2011.

Figure 6. The Insightec ExAblate™ Neuro MRI-Guided Focused Ultrasound Surgical System. Credit: MR Center, University Children's Hospital Zurich. Copyright Journal of Neurosurgery Publishing Group (JNSPG) 2012.

accurately target a multi-element phased ultrasound array at the same location as the (simulated) point source. Early numerical simulations of the human skull and brain required several hours (sometimes days) to complete, motivating the development of computationally efficient alternatives to full FDTD or finite element method simulations using ray acoustics and angular spectrum simulation. Both approaches follow simple, plane wave propagation physics, with the angular spectrum approach also capturing diffraction effects; hybrid combinations of these approaches are also possible. Computationally efficient approaches allow substantial reductions in both the time and computer resources required, and have led in recent years to accurate, personalized targeting solutions for transcranial ultrasound focusing using several different strategies, including multi-domain algorithms to minimize skull heating and the focal region extent (Pulkkinen *et al* 2011), accurate and efficient angular spectrum methods for inhomogeneous media (Vyas and Christensen 2012) and a 'phase only' ray acoustics/FDTD hybrid approach to the transcranial ultrasound problem (Pinton

et al 2012c), yielding similar accuracy results in one quarter of the time, using half the computational resources, as the full FDTD simulation baseline.

Within the past decade, the efficacy of US phased array systems and their associated numerical targeting algorithms to accurately and non-invasively target millimeter-scale neural structures within the human cranium has been experimentally validated and clinically demonstrated in hundreds of patients. Since the major technical issues hindering widespread use of these tools for neurosurgery have been mostly resolved, much of the recent work in this area examines optimization factors, such as the effects of skull properties and even scalp hair on the ultrasonic focal region (Raymond and Hynynen 2005, Eames *et al* 2014), and improving the prediction of resulting sonication outcomes. These advances provide a demonstration of what is possible for ultrasonic beam-forming within the human cranium, and a benchmark for estimating the targeting efficacy of future ultrasound neuromodulation systems. Because HIFU intensities are about 2–3 orders of magnitude higher than neuromodulation intensities, it is widely expected that these targeting solutions can be readily applied for neuromodulation to achieve similar accuracy and resolution by attenuating the transmitted power and adjusting the waveform to achieve a desired effect.

Safety considerations

A key constraint shaping the work of researchers, clinicians, and equipment developers is the long-term safety of ultrasonic neuromodulation treatment protocols. There is a well-developed field of knowledge concerning the biological damage potential of US. Consequently, compliance metrics have been mandated by the FDA and other regulatory agencies (AIUM, NEMA) for clinical ultrasound imaging and therapeutic systems. Guidelines usually include limitations on the MI, thermal index and spatial peak time average intensity (I_{spta}). These should be treated as minimum requirements, since safety concerns (and eventual device approvals—see emerging clinical and research applications in the discussion section) will be based upon regulations already in place concerning the benign operation of non-surgical ultrasound equipment.

Investigators in this field, well aware of these guidelines, often detail at least the MI and I_{spta} of the experimental stimulation protocols (e.g. Tufail *et al* 2010, Naor *et al* 2012, Kim *et al* 2014a), and thus it is clear that efficient neuromodulation in anesthetized small animals is attainable within the accepted safety guidelines (for humans). In some studies the safety was also directly examined (Yoo *et al* 2011a, Naor *et al* 2012, Kim *et al* 2014a), and the investigators reported that there were no signs of structural damage to the tissue.

Discussion and outlook

The rapidly increasing body of findings surveyed above already provides ample empirical evidence that US waves can flexibly modulate the function of neural circuits; combined with advanced focusing technologies, it should be apparent that US neuromodulation technology has a unique potential for non-invasive and spatially confined influence on both deep and relatively superficial neural structures. The major practical challenges and limitations associated with experimental examination of US neuromodulation (e.g., electrode mechanical artefacts and stability, strong anesthesia effects, standing waves within the skull, etc) has led the researchers in this field to apply and study a wide range of experimental preparations and protocols. Effects were broadly observed using either modulatory excitation protocols lasting many seconds to minutes or, as explored more recently, driven causally by punctate and direct stimuli lasting tens to hundreds of milliseconds: in cortex, excitation appears to be elicited when the pulses are nearly continuous while suppression seems to be favored by short and discontinuous pulses. These timescales are orders-of-magnitude slower than those needed for direct electrical or optical stimulation, suggesting that the mechanism of action is indirect; although potentially very interesting, to date there are only scattered anecdotal reports that ms-timescale stimuli can elicit such responses. In contradistinction to the effects mediated over CNS neuronal populations, studies on the interaction of US with nerve (axonal) bundles have mostly outlined a relatively weak parametric effect on propagation parameters in the exposed segment, which was mostly suppressive and often long-lasting. Initial recent evidence for direct US *stimulation* in the rat abducens (Kim *et al* 2012) and the *ex vivo* crab leg (Wright *et al* 2015) nerves are potentially interesting but do not yet provide unequivocal support for this mode of interaction. Finally, it is also interesting to note that typical US intensities used to obtain neuromodulatory effects correspond to peak pressure amplitudes of roughly 3–5 atmospheres (~3–7.5 W cm^{-2} intensities), which may have an indirect correspondence to the type of pressure perturbations that cause biological effects such as decompression sickness.

Below, we survey research trends and emerging applications, as well as gaps and challenges.

Biophysical mechanisms underlying ultrasonic neuromodulation

The empirical success in demonstrating causal neural stimulation and inhibition using low intensity ultrasound has prompted research into possible mechanisms of action. While the effect is clearly primarily mechanical, US exerts multiple modes of mechanical interactions on tissues and their boundaries (discussed briefly in the *Primer*) and it is important to understand which specific effects dominate here, what are the target cellular structures and how they transduce this interaction, and to ultimately capture the underlying biophysics. Early attempts by Tyler to deduce the mode of interaction includes a pharmacological dissection of the excitations observed in Tyler *et al* (2008) using specific blockers, leading to a tentative conclusion that sodium channels are the mediators of the acoustic effect; however, the analysis did not separate direct US transduction from their trivial involvement in action-potential generation. In a later

qualitative theoretical analysis, Tyler (2011) uses estimates of the Knudsen number ($\ll 1$) for typical biological systems to rule out the involvement of statistical quantum mechanical effects in ultrasonic neuromodulation, proposing instead a general fluid-dynamics type 'continuum mechanics hypothesis' for studying and modeling the complex interactions of ultrasonic waveforms with neural tissues.

Several authors have highlighted the potential role of radiation pressure in eliciting ultrasonic neuromodulation. Wahab *et al* (2012) observed reductions in the amplitude and conduction velocity of electrically evoked action potentials elicited by earthworm's giant axon after sonicating them with acoustic impulse trains. With acoustic intensities below the cavitation thresholds or physiologically significant temperature elevations, changes were found to be in good correlation with the *cumulative radiation force*, suggesting a causative role for acoustic radiation force effects in modulating (suppressing) nervous system activity. Prieto *et al* (2013) later reached a similar conclusion by electrophysiologically studying the dynamic response to US of model (isolated) lipid membranes. However, the presence of complex boundary and gradient forces in the experimental setup complicates this interpretation, and may actually lead to an opposite conclusion regarding the role of radiation force in US brain stimulation (Plaksin *et al* manuscript in preparation).

A novel, alternative mode of US-tissue interaction proposed and studied by Kimmel, Shoham and colleagues involves *intramembrane cavitation*, or localized cavitation within the bilipid cell membrane in response to applied ultrasound (Krasovitski *et al* 2011). The proposed 'BiLayer Sonophore' (BLS) model predicts that many of the non-thermal bioeffects of ultrasound observed both in tissue cultures and *in vivo* could stem from the generation of nanometric bubbles within the bilipid membranes surrounding practically all living cells. These nanobubbles appear and fluctuate as discrete pockets within the phospholipid bilayer, stitched together by transmembrane proteins, when negative acoustic pressure transiently overcomes the attraction forces binding the membrane's phospholipid leaflets. Utilizing the bubble mechanics mathematical framework to calculate dynamic geometric changes in the cellular membrane, the model predicts a spectrum of increasingly acute and biologically plausible effects to increasing US intensities, up to the formation of nanometric pores compatible with observed increases in membrane permeability. In follow-up work, the effect of these BLS-based bilayer membrane vibrations on the electrical behavior of excitable CNS tissues was studied using a neuronal intramembrane cavitation excitation (NICE) framework (Plaksin *et al* 2014), by examining the direct and indirect effects of membrane capacitance fluctuations they induce. When NICE model membranes are sonicated, the rapid capacitance oscillations lead to hyperpolarizing displacement currents ($\propto V \cdot \mathrm{d}C/\mathrm{d}t$) whose interplay with the cell's passive and active conductances ultimately leads to indirect excitation and firing of action potentials. The model-based neuronal response predictions were found to be both qualitatively and quantitatively consistent with the experimental evidence.

Taken together, while there is as yet no *direct* biophysical evidence underpinning a mechanistic understanding of specific US neuromodulation phenomena, major research efforts undertaken in this area are increasingly turning it into an area of rigorous scientific investigation. Understanding the specific biophysics of US neuromodulation has turned out to be highly nontrivial. Neuromodulation may be mediated through more than one mechanism and multiple regimes and mechanisms may co-exist in a particular experiment (with varying relative importance). Experimental measurements are also challenging: (1) electrical currents are not directly induced into the target tissue; (2) US waves have a microsecond timescale; (3) US tends to mechanically disrupt patch-electrode seals (Tyler *et al* 2008) and is generally ill adapted for study in existing electrophysiology chambers (due to wall reflections). It is therefore not less important to recognize and consolidate the emerging lines of *indirect* evidence. For example, it has become increasingly likely that capacitive displacement currents are the major players in US neuromodulation since their emergence is predicted both as a result of radiation-pressure-induced dynamic membrane bending (Prieto *et al* 2013) and by the NICE framework (Plaksin *et al* 2014) (capacitive currents may also underlie thermal neuro-stimulation, as per Shapiro *et al* 2012). In the absence of direct measurements, theoretical frameworks can be evaluated by testing their qualitative and quantitative predictions. NICE response predictions have so far been found to be consistent with detailed parametric measurements of activation by mouse motor cortical stimulation (King *et al* 2013), where it also explained the requirement for long stim durations, suboptimal performance of CW waveforms and the paradoxical observations of strong dependence on frequency. In follow-up work, it was further shown to predict the emergence of cortical neural suppression and to suggest plausible insights into both the mechanisms and the stimulation parameter space (Plaksin *et al*, manuscript in review).

Biophysical strategies for improved targeting

US neuromodulation currently mostly relies on relatively low-frequencies ($\leqslant 1$ MHz) and practically requires high-end systems to provide mm-scale spatial confinement of the modulatory effect. This targeting capability may be comparable to that of electrical stimulation, but is still limited when compared to (higher frequency) US diagnostic imaging or the cell-type selective optical neuromodulation. Novel approaches to improve selectivity aspects of US neuromodulation are thus highly desirable, and strategies based on waveform modulation and localized field enhancement are being pursued.

Mehic *et al* (2014) describe an attempt to improve the focal properties of ultrasonic neuromodulation using modulated FUS, a technique borrowed from vibro-acoustography wherein a high frequency carrier beam is focused while maintaining the essential effect of a lower frequency stimulus (the AM signal envelope). The approach relies on combining two high-frequency beams (1.75 and 2.25 MHz) to result in a low-frequency (0.5 MHz) component that would effectively

modulate the tissue. However, this combination strongly relies on a nonlinear effect (presumably radiation pressure) being the key driver of US neuromodulation, and only minor disparities in regional efficacy are actually demonstrated in Mehic *et al* (2014) for the modulated versus unmodulated (2 MHz) sonications.

Another promising direction comes from the developing field of targeted contrast-enhanced ultrasound (Lanza *et al* 1996, Deshpande *et al* 2010), potentially providing improvements in both spatial resolution and cell-type specificity. In this approach, targeting ligands that bind to specific cell membrane receptors are chemically bound (conjugated) to gas microbubbles–an acoustically reactive element. The selective accumulation of this complex in regions/tissue types of interest could potentially address focusing limitations inherent in low-frequency US neuromodulation, as the presence of the microbubbles is expected to permit neuronal stimulation at much lower ultrasonic intensities. Indeed, a very recent method explored the highly related use of the natural large-pore nanobubble in the protein TRP4 for eliciting cell-type selective 'sono-genetic' excitation of specific neurons in the nematode *C. elegans* (Ibsen *et al* 2015).

A different, recently demonstrated targeting scheme relies on focal transfer of systemically administered neuromodulatory compounds by US BBB disruption. Shown to effectively modulate the neural response by itself (McDannold *et al* 2015), the combination of this relatively slow approach with the dynamic, direct US neuromodulation approach has the potential to improve the effective spatial confinement, while retaining the rapid sub-second modulation timescale.

The issue of cell-type-selective excitation is clearly one of the hallmarks of modern neural science and technology and its realization using exogenous or endogenous tools is particularly interesting in the context of this non-invasive modality. As discussed above, selective excitation and suppression based on the pulse parameters defining the sonication stimulus is well established (Kim *et al* 2015) but poorly understood; recent predictions from the NICE model provide a comprehensive explanation of these effects as resulting from US parameter-based cell-type selective excitation (Plaksin *et al*, unpublished analyses).

Multifocal stimulation

Algorithms for simultaneous generation of distributed acoustic targets containing multiple focal points in an US field were first described in (Ebbini and Cain 1989, Ibbini and Cain 1989), in the context of time-effective hyperthermia treatments; the latter 'pseudo-inverse' method was further developed and studied by several groups (Wang *et al* 1990, Ebbini and Cain 1991, Lalonde *et al* 1993, Botros *et al* 1997, Wu and Sherar 2002). Studies by Gavrilov and colleagues, aimed at optimizing phased array designs (Gavrilov and Hand 2000, Hand *et al* 2009) later considered multi-focal US as a technology for 'transmission of sensory information transfer to a human', e.g. as dynamic tactile Braille displays (Gavrilov 2008).

In recent work, we proposed and began to explore the potential that multifocal simultaneous patterned acoustic neuromodulation could have for flexible spatio-temporal control of multiple neural targets, inspired by closely related work in patterned photo-control of neural circuits (Golan *et al* 2009, Reutsky-Gefen *et al* 2013). To address this challenge, we introduced new patterning techniques by extending and adapting computational techniques from the field of optical computer generated holography, and demonstrated their ability to synthesize complex, coherent ultrasonic interference patterns in an ultrasound 'phantom', utilizing a high density (987 element) ultrasonic phased array driven by a 2.3 MHz source frequency (Hertzberg *et al* 2010, Naor *et al* 2012). See figure 4, panel (e) for details.

Emerging clinical and research applications

The potential of non-invasively stimulating excitable tissues within the CNS with ultrasound is inspiring researchers to explore novel medical applications and procedures. In general, many of the neurological disorders currently treated or suggested as treatable with electrode-based deep brain stimulation (Chen *et al* 2013, Williams and Okun 2013, Kocabicak *et al* 2015), TMS systems (Rossini *et al* 2015) and related modalities could potentially be viable candidates for non-invasive treatment via ultrasonic neuromodulation. In a recent meeting, the Focused Ultrasound Foundation's NeuroModulation Workgroup identified pre-surgical mapping, functional brain mapping, non-destructive suppression of neural disorders, and non-invasive treatment of pain as research concerns with the highest clinical utility and/or therapeutic benefit (FUSF 2014). Although the energetic cost of ultrasonically eliciting action potentials from neurons is several orders of magnitude higher than what is typically required with electrode based systems (Plaksin *et al* 2014), the potential elimination of the surgical risk and cumulative tissue damage inherent in electrode-based treatments could more than compensate the increased expected 'battery drain'. Moreover, as the currently available MRgFUS systems were designed for ablation surgery, they can support intensities several orders of magnitude higher than required for US neuromodulation and future neuromodulation systems can relax many related design constraints, hopefully leading to reductions in the costs.

The broad spectrum of potential applications of future US neuromodulation tools could also include closed-loop modulation strategies, similar to those already pursued by researchers developing HIFU-based tools for effective emergency cardiac pacing following cardiac arrest (Livneh *et al* 2014), as well as those afforded by 'dual mode' US imaging/thermography + stimulation/treatment array systems (Haritonova *et al* 2015). Solutions based on lightweight, *portable* devices will proliferate as researchers investigate the viability of translating experimental 'wins' from ad hoc laboratory systems into tightly integrated, user-friendly hardware platforms. One example is artificial vision restoration using acoustic retinal prostheses (Hertzberg *et al* 2010, Naor *et al* 2012, Menz *et al* 2013) that will

combine multifocal acoustic pattern generation techniques and US retinal stimulation. The non-invasive nature of such a portable instrument renders it an attractive alternative to implantable electrode based retinal prosthetics, and it will be interesting to explore additional applications with similar characteristics. Notably, although the review primarily highlights the state-of-the-art and potential for rapid US neuromodulation of CNS neurons, the potential value of non-invasive modulation of nerves should also not be underestimated, including, e.g., temporary nerve block for pain management or drug-free anesthesia (Lee *et al* 2015b), and autonomic neuromodulation for applications ranging from neuromuscular deficits, to reduction of cardiac arrhythmogenesis, and even to chronic gastric problems.

Finally, ultrasonic neuromodulation holds great potential as a basic research tool. Refined targeting procedures that will limit the effective field of ultrasonic neuromodulation, will provide neuroscientists with a reversible and non-invasive means to 'turn on' or block selective segments of neural circuits in animals and humans. Coupled with non-invasive functional imaging approaches, this capability to modulate specific neural processes will give researchers new insights into the activities and interdependencies of *in vivo* neural networks. Ultrasonic entrainment of specific neural segments might provide a means of correcting dysfunction or even enhancing performance within the nervous system, providing neuroscientists, engineers and clinical scientists with exciting new avenues of research.

Acknowledgments

The authors thank Eilon Hazan, Josh Nehrer, Michael Plaksin, and Dr Dan Adam for their comments on the manuscript. The work was supported by the Israel Science Foundation (ISF grant no. 1725/13) and the BSMT Consortium from the Office of the Chief Scientist [OCS] in Israel's Ministry of Economy.

References

Adrianov O S, Vykhodtseva N I, Fokin V F, Uranova N A, Avirom V M and Galogazha M 1984 Reversible functional blocking of the optic tract by focused ultrasound *Bull. Exp. Biol. Med.* **97** 844–7

Altberg W 1903 Uber die druckkrafte der schallwellen und die absolute messung der schallintensitat *Ann. Phys., Lpz.* **11** 405–20

Aryal M, Arvanitis C D, Alexander P M and McDannold N 2014 Ultrasound-mediated blood–brain barrier disruption for targeted drug delivery in the central nervous system *Adv. Drug Deliv. Rev.* **72** 94–109

Azhari H 2010 *Basics of Biomedical Ultrasound for Engineers* (Hoboken, NJ: Wiley-IEEE Press)

Bachtold M R, Rinaldi P C, Jones J P, Reines F and Price L R 1998 Focused ultrasound modifications of neural circuit activity in a mammalian brain *Ultrasound Med. Biol.* **24** 557–65

Ballantine H T Jr, Bell E and Manlapaz J 1960 Progress and problems in the neurological applications of focused ultrasound *J. Neurosurg.* **17** 858–76

Bamber J C 1998 Ultrasonic properties of tissue *Ultrasound in Medicine* ed F A Duck *et al* (Boca Raton, FL: CRC Press)

Botros Y Y, Volakis J L, VanBaren P and Ebbini E S 1997 A hybrid computational model for ultrasound phased-array heating in presence of strongly scattering obstacles *IEEE Trans. Biomed. Eng.* **44** 1039–50

Bystritsky A, Korb A S, Douglas P K, Cohen M S, Melega W P, Mulgaonkar A P, DeSalles A, Min B K and Yoo S S 2011 A review of low-intensity focused ultrasound pulsation *Brain Stimul.* **4** 125–36

Carstensen E L, Child S Z, Norton S and Nyborg W 1990 Ultrasonic heating of the skull *J. Acoust. Soc. Am.* **86** S29–29

Chen X L, Xiong Y Y, Xu G L and Liu X F 2013 Deep brain stimulation *Interventional Neurology* **1** 200–12

Colucci V, Strichartz G, Jolesz F, Vykhodtseva N and Hynynen K 2009 Focused ultrasound effects on nerve action potential in vitro *Ultrasound Med. Biol.* **35** 1737–47

Deffieux T, Younan Y, Wattiez N, Tanter M, Pouget P and Aubry J F 2013 Low-intensity focused ultrasound modulates monkey visuomotor behavior *Curr. Biol.* **23** 2430–3

Deshpande N, Needles A and Willmann J K 2010 Molecular ultrasound imaging: current status and future directions *Clin. Radiol.* **65** 567–81

Eames M D, Hananel A, Snell J W, Kassell N F and Aubry J F 2014 Trans-cranial focused ultrasound without hair shaving: feasibility study in an ex vivo cadaver model *J. Ther. Ultrasound* **1** 24

Ebbini E S and Cain C A 1989 Multiple-focus ultrasound phased-array pattern synthesis: optimal driving-signal distributions for hyperthermia *IEEE Trans. Ultrason. Ferroelectr. Freq. Control* **36** 540–8

Ebbini E S and Cain C A 1991 A spherical-section ultrasound phased array applicator for deep localized hyperthermia *IEEE Trans. Biomed. Eng.* **38** 634–43

Fatemi M and Greenleaf J F 1998 Ultrasound-stimulated vibro-acoustic spectrography *Science* **280** 82–5

Foster K R and Wiederhold M L 1978 Auditory responses in cats produced by pulsed ultrasound *J. Acoust. Soc. Am.* **63** 1199–205

Fry F J, Ades H W and Fry W J 1958 Production of reversible changes in the central nervous system by ultrasound *Science* **127** 83–4

Fry F J and Barger J E 1978 Acoustical properties of the human skull *J. Acoust. Soc. Am.* **63** 1576–90

Fry W J, Mosberg W H Jr, Barnard J W and Fry F J 1954 Production of focal destructive lesions in the central nervous system with ultrasound *J. Neurosurgery* **11** 471–8

FUSF Focused Ultra Sound Foundation, Neuromodulation Workgroup 2014 *FUSF White Paper: Neuromodulation Workshop* Retrieved from:(http://fusfoundation.org/images/pdf/NM_workshop_whitepaper_alphaorder.pdf)

Gavrilov L R 2008 The possibility of generating focal regions of complex configurations in application to the problems of stimulation of human receptor structures by focused ultrasound *Acoust. Phys.* **54** 269–78

Gavrilov L R 2014 *Use of Focused Ultrasound for Stimulation of Various Neural Structures* (New York: Nova Science Publishers)

Gavrilov L R, Gersuni G V, Ilyinski O B, Tsirulnikov E M and Shchekanov E E 1977a A study of reception with the use of focused ultrasound. I. Effects on the skin and deep receptor structures in man *Brain Res.* **135** 265–77

Gavrilov L R, Gersuni G V, Ilyinsky O B, Tsirulnikov E M and Shchekanov E E 1977b A study of reception with the use of focused ultrasound. II. Effects on the animal receptor structures *Brain Res.* **135** 279–85

Gavrilov L R and Hand J W 2000 A theoretical assessment of the relative performance of spherical phased arrays for ultrasound surgery *IEEE Trans. Ultrason. Ferroelectr. Freq. Control* **47** 125–39

Gavrilov L R and Tsirulnikov E M 2012 Focused ultrasound as a tool to input sensory information to humans (review) *Acoust. Phys.* **58** 1–21

Gavrilov L R, Tsirulnikov E M and Davies I A 1996 Application of focused ultrasound for the stimulation of neural structures *Ultrasound Med. Biol.* **22** 179–92

Golan L, Reutsky I, Farah N and Shoham S 2009 Design and characteristics of holographic neural photo-stimulation systems *J. Neural Eng.* **6** 066004

Hameroff S, Trakas M, Duffield C, Annabi E, Gerace M B, Boyle P, Lucas A, Amos Q, Buadu A and Badal J J 2013 Transcranial ultrasound (TUS) effects on mental states: a pilot study *Brain Stimul.* **6** 409–15

Hand J W, Shaw A, Sadhoo N, Rajagopal S, Dickinson R J and Gavrilov L R 2009 A random phased array device for delivery of high intensity focused ultrasound *Phys. Med. Biol.* **54** 5675

Haritonova A, Liu D and Ebbini E S 2015 In vivo application and localization of transcranial focused ultrasound using dual-mode ultrasound arrays *IEEE Trans. Ultrason. Ferroelectr. Freq. Control* **62** 2031–42

Harvey E N 1929 The effect of high frequency sound waves on heart muscle and other irritable tissues *Am. J. Physiol.—Legacy Content* **91** 284–90

Hertzberg Y, Naor O, Volovick A and Shoham S 2010 Towards multifocal ultrasonic neural stimulation: pattern generation algorithms *J. Neural. Eng.* **7** 056002

Hölscher T, Fisher D J, Raman R, Ernstrom K, Zadicario E, Bradley W G and Voie A 2011 Noninvasive transcranial clot lysis using high intensity focused ultrasound *J. Neurol. Neurophysiol. S1*

Hynynen K and Jolesz F A 1998 Demonstration of potential noninvasive ultrasound brain therapy through an intact skull *Ultrasound Med. Biol.* **24** 275–83

Ibbini M S and Cain C A 1989 A field conjugation method for direct synthesis of hyperthermia phases-array heating patterns *IEEE Trans. Ultrason. Ferroelectr. Freq. Control* **36** 3–9

Ibsen S, Tong A, Schutt C, Esener S and Chalasani S H 2015 Sonogenetics is a non-invasive approach to activating neurons in caenorhabditis elegans *Nat. Commun.* **6** 8264

Jagannathan J, Sanghvi N K, Crum L A, Yen C-P, Medel R, Dumont A S, Sheehan J P, Steiner L, Jolesz F and Kassell N F 2009 High intensity focused ultrasound surgery (HIFU) of the brain: a historical perspective, with modern applications *Neurosurgery* **64** 201–11

Jolesz F A and Hynynen K 2008 *MRI-Guided Focused Ultrasound Surgery* (New York: Informa Healthcare)

Juan E J, Gonzalez R, Albors G, Ward M P and Irazoqui P 2014 Vagus nerve modulation using focused pulsed ultrasound: potential applications and preliminary observations in a rat *Int. J. Imaging Syst. Technol.* **24** 67–71

Kamimura H, Wang S, Chen H, Wang Q, Aurup C, Acosta C, Carneiro A and Konofagou E 2015 Pupil dilation and motor response elicitation by ultrasound neuromodulation *2015 IEEE Int. Ultrasonics Symp. (IUS)* pp 1–4

Kim H, Chiu A, Lee S D, Fischer K and Yoo S S 2014a Focused ultrasound-mediated non-invasive brain stimulation: examination of sonication parameters *Brain Stimul.* **7** 748–56

Kim H, Lee S D, Chiu A, Yoo S S and Park S 2014b Estimation of the spatial profile of neuromodulation and the temporal latency in motor responses induced by focused ultrasound brain stimulation *Neuroreport* **25** 475–9

Kim H, Park M Y, Lee S D, Lee W, Chiu A and Yoo S S 2015 Suppression of EEG visual-evoked potentials in rats through neuromodulatory focused ultrasound *Neuroreport* **26** 211–5

Kim H, Taghados S J, Fischer K, Maeng L-S, Park S and Yoo S S 2012 Noninvasive transcranial stimulation of rat abducens nerve by focused ultrasound *Ultrasound Med. Biol.* **38** 1568–75

King R L, Brown J R, Newsome W T and Pauly K B 2013 Effective parameters for ultrasound-induced *in vivo* neurostimulation *Ultrasound Med. Biol.* **39** 312–31

King R L, Brown J R and Pauly K B 2014 Localization of ultrasound-induced in vivo neurostimulation in the mouse model *Ultrasound Med. Biol.* **40** 1512–22

Kocabicak E, Temel Y, Hollig A, Falkenburger B and Tan S K H 2015 Current perspectives on deep brain stimulation for severe neurological and psychiatric disorders *Neuropsychiatric Disease Treat.* **11** 1051–66

Konofagou E E, Tung Y-S, Choi J, Deffieux T, Baseri B and Vlachos F 2012 Ultrasound-induced blood–brain barrier opening *Theranostics* **13** 1223–37

Koroleva V I, Vykhodtseva N I and Elagin V A 1986 Cortical and subcortical spreading depression in rats produced by focused ultrasound *Neurophysiology* **18** 43–8

Krasovitski B, Frenkel V, Shoham S and Kimmel E 2011 Intramembrane cavitation as a unifying mechanism for ultrasound-induced bioeffects *Proc. Natl Acad. Sci. USA* **108** 3258–63

Lalonde R J, Worthington A and Hunt J W 1993 Field conjugate acoustic lenses for ultrasound hyperthermia *IEEE Trans. Ultrason. Ferroelectr. Freq. Control* **40** 592–602

Lanza G M, Wallace K D, Scott M J, Cacheris W P, Abendschein D R, Christy D H, Sharkey A M, Miller J G, Gaffney P J and Wickline S A 1996 A novel site-targeted ultrasonic contrast agent with broad biomedical application *Circulation* **94** 3334–40

Lee C P and Wang T G 1993 Acoustic radiation pressure *J. Acoust. Soc. Am.* **94** 1099–109

Lee W, Kim H, Jung Y, Song I U, Chung Y A and Yoo S S 2015 Image-guided transcranial focused ultrasound stimulates human primary somatosensory cortex *Sci. Rep.* **5** 8743

Lee W, Lee S D, Park M Y, Foley L, Purcell-Estabrook E, Kim H, Fischer K, Maeng L S and Yoo S S 2016 Image-guided focused ultrasound-mediated regional brain stimulation in sheep *Ultrasound Med. Biol.* **42** 459–70

Lee Y F, Lin C C, Cheng J S and Chen G S 2015b Nerve conduction block in diabetic rats using high-intensity focused ultrasound for analgesic applications *Br. J. Anaesthesia* **114** 840–6

Legon W, Sato T F, Opitz A, Mueller J, Barbour A, Williams A and Tyler W J 2014 Transcranial focused ultrasound modulates the activity of primary somatosensory cortex in humans *Nat. Neurosci.* **17** 322–9

Lele P P 1963 Effects of focused ultrasonic radiation on peripheral nerve, with observations on local heating *Exp. Neurology* **8** 47–83

Lindstrom P A 1954 Prefrontal ultrasonic irradiation—a substitute for lobotomy *AMA Arch. Neurology Psychiatry* **72** 399–425

Livneh A, Kimmel E, Kohut A R and Adam D 2014 Extracorporeal acute cardiac pacing by high intensity focused ultrasound *Prog. Biophys. Mol. Biol.* **115** 140–53

Lynn J G, Zwemer R L, Chick A J and Miller A E 1942 A new method for the generation and use of focused ultrasound in experimental biology *J. Gen. Physiol.* **26** 179–93

McDannold N, King R L and Hynynen K 2004 MRI monitoring of heating produced by ultrasound absorption in the skull: in vivo study in pigs *Magn. Reson. Med.* **51** 1061–5

McDannold N, Zhang Y-Z, Power C, Arvanitis C, Vykhodtseva N and Livingstone M 2015 Targeted delivery of GABA via ultrasound-induced blood–brain barrier disruption blocks somatosensory-evoked potentials *J. Therapeutic Ultrasound* **3** P28

Mehic E, Xu J M, Caler C J, Coulson N K, Moritz C T and Mourad P D 2014 Increased anatomical specificity of neuromodulation via modulated focused ultrasound *PLoS One* **9** e86939

Menz M D, Oralkan O, Khuri-Yakub P T and Baccus S A 2013 Precise neural stimulation in the retina using focused ultrasound *J. Neurosci.* **33** 4550–60

Mihran R T, Barnes F S and Wachtel H 1990 Temporally-specific modification of myelinated axon excitability in vitro following a single ultrasound pulse *Ultrasound Med. Biol.* **16** 297–309

Min B K, Bystritsky A, Jung K I, Fischer K, Zhang Y, Maeng L S, Park S I, Chung Y A, Jolesz F A and Yoo S S 2011a Focused ultrasound-mediated suppression of chemically-induced acute epileptic EEG activity *BMC Neurosci.* **12** 23

Min B K, Yang P S, Bohlke M, Park S, Vago R D, Maher T J and Yoo S S 2011b Focused ultrasound modulates the level of cortical neurotransmitters: potential as a new functional brain mapping technique *Int. J. Imaging Syst. Technol.* **21** 232–40

Morse P and Ingard K 1987 *Theoretical Acoustics* (Princeton, NJ: Princeton University Press)

Mueller J, Legon W, Opitz A, Sato T F and Tyler W J 2014 Transcranial focused ultrasound modulates intrinsic and evoked EEG dynamics *Brain Stimul.* **7** 900–8

Muratore R, LaManna J, Szulman E, Kalisz M S A, Lamprecht M, Simon M S M, Yu M S Z, Xu N and Morrison B 2009 Bioeffective ultrasound at very low doses: reversible manipulation of neuronal cell morphology and function in vitro *AIP Conf. Proc.* **1113** 25–9 (paper presented in 2008)

Naor O, Hertzberg Y, Zemel E, Kimmel E and Shoham S 2012 Towards multifocal ultrasonic neural stimulation II: Design considerations for an acoustic retinal prosthesis *J. Neural Eng.* **9** 026006

Nelson T R, Fowlkes J B, Abramowicz J S and Church C C 2009 Ultrasound biosafety considerations for the practicing sonographer and sonologist *J. Ultrasound Med.* **28** 139–50

O'Reilly M A, Muller A and Hynynen K 2011 Ultrasound insertion loss of rat parietal bone appears to be proportional to animal mass at submegahertz frequencies *Ultrasound Med. Biol.* **37** 1930–7

Pinton G, Aubry J F, Bossy E, Muller M, Pernot M and Tanter M 2012a Attenuation, scattering, and absorption of ultrasound in the skull bone *Med. Phys.* **39** 299–307

Pinton G, Aubry J F, Fink M and Tanter M 2012b Numerical prediction of frequency dependent 3D maps of mechanical index thresholds in ultrasonic brain therapy *Med. Phys.* **39** 455–67

Pinton G F, Aubry J F and Tanter M 2012c Direct phase projection and transcranial focusing of ultrasound for brain therapy *IEEE Trans. Ultrason. Ferroelectr. Freq. Control* **59** 1149–59

Plaksin M, Shoham S and Kimmel E 2014 Intramembrane cavitation as a predictive bio-piezoelectric mechanism for ultrasonic brain stimulation *Phys. Rev.* X **4** 011004

Prieto M L, Oralkan O, Khuri-Yakub B T and Maduke M C 2013 Dynamic response of model lipid membranes to ultrasonic radiation force *PLoS One* **8** e77115

Pulkkinen A, Huang Y, Song J and Hynynen K 2011 Simulations and measurements of transcranial low-frequency ultrasound therapy: skull-base heating and effective area of treatment *Phys. Med. Biol.* **56** 4661–83

Raymond S B and Hynynen K 2005 Acoustic transmission losses and field alterations due to human scalp hair *IEEE Trans. Ultrason. Ferroelectr. Freq. Control* **52** 1415–9

Reutsky-Gefen I, Golan L, Farah N, Schejter A, Tsur L, Brosh I and Shoham S 2013 Holographic optogenetic stimulation of patterned neuronal activity for vision restoration *Nat. Commun.* **4** 1509

Rinaldi P C, Jones J P, Reines F and Price L R 1991 Modification by focused ultrasound pulses of electrically evoked responses from an in vitro hippocampal preparation *Brain Res.* **558** 36–42

Rossini P M *et al* 2015 Non-invasive electrical and magnetic stimulation of the brain, spinal cord, roots and peripheral nerves: basic principles and procedures for routine clinical and research application an updated report from an IFCN committee *Clin. Neurophysiology* **126** 1071–107

Shapiro M G, Homma K, Villarreal S, Richter C-P and Bezanilla F 2012 Infrared light excites cells by changing their electrical capacitance *Nat. Commun.* **3** 736

Takagi S F, Higashino S, Shibuya T and Osawa N 1960 The actions of ultrasound on the myelinated nerve, the spinal cord and the brain *Japan. J. Physiology* **10** 183–93

Thomas J-L and Fink M A 1996 Ultrasonic beam focusing through tissue inhomogeneities with a time reversal mirror: application to transskull therapy *IEEE Trans. Ultrason. Ferroelect. Freq. Control* **43** 1122–9

Torr G R 1984 The acoustic radiation force *Am. J. Phys.* **52** 402–8

Tsirulnikov E M, Vartanyan I A, Gersuni G V, Rosenblyum A S, Pudov V I and Gavrilov L R 1988 Use of amplitude-modulated focused ultrasound for diagnosis of hearing disorders *Ultrasound Med. Biol.* **14** 277–85

Tufail Y, Matyushov A, Baldwin N, Tauchmann M L, Georges J, Yoshihiro A, Tillery S I and Tyler W J 2010 Transcranial pulsed ultrasound stimulates intact brain circuits *Neuron* **66** 681–94

Tyler W J 2011 Noninvasive neuromodulation with ultrasound? A continuum mechanics hypothesis *Neuroscientist* **17** 25–36

Tyler W J, Tufail Y, Finsterwald M, Tauchmann M L, Olson E J and Majestic C 2008 Remote excitation of neuronal circuits using low-intensity, low-frequency ultrasound *PLoS One* **3** e3511

Velling V A and Shklyaruk S P 1988 Modulation of the functional state of the brain with the aid of focused ultrasonic action *Neurosci. Behav. Physiol.* **18** 369–75

Vyas U and Christensen D 2012 Ultrasound beam simulations in inhomogeneous tissue geometries using the hybrid angular spectrum method *IEEE Trans. Ultrason. Ferroelectr. Freq. Control* **59** 1093–100

Vykhodtseva N and Konopatskaya I 2007 Focused ultrasound potential to initiate spreading depression for disruption of blood brain barrier *2007 IEEE Ultrasonics Symp.* pp 428–31

Vykhodtseva N I and Koroleva V I 2006 Steady potential changes and spreading depression in rat brains produced by focused ultrasound *AIP Conf. Proc.* **829** 59–63

Wahab R A, Choi M, Liu Y, Krauthamer V, Zderic V and Myers M R 2012 Mechanical bioeffects of pulsed high intensity focused ultrasound on a simple neural model *Med. Phys.* **39** 4274–83

Wang H, Ebbini E and Cain C A 1990 Computationally efficient algorithms for control of ultrasound phased-array hyperthermia applicators based on a pseudoinverse method *IEEE Trans. Ultrason. Ferroelectr. Freq. Control* **37** 274–7

Westervelt P J 1951 The theory of steady forces caused by sound waves *J. Acoust. Soc. Am.* **23** 312–5

White J, Clement G T and Hynynen K 2005 Transcranial ultrasound focus reconstruction with phase and amplitude correction *IEEE Trans. Ultrason. Ferroelectr. Freq. Control* **52** 1518–22

Williams N R and Okun M S 2013 Deep brain stimulation (DBS) at the interface of neurology and psychiatry *J. Clin. Investigation* **123** 4546–56

Wright C J, Rothwel J and Saffari N 2015 Ultrasonic stimulation of peripheral nervous tissue: an investigation into mechanisms *J. Phys.: Conf. Ser.* **581** 012003

Wu X and Sherar M 2002 Theoretical evaluation of moderately focused spherical transducers and multi-focus acoustic lens/transducer systems for ultrasound thermal therapy *Phys. Med. Biol.* **47** 1603

Yang P S, Kim H, Lee W, Bohlke M, Park S, Maher T J and Yoo S S 2012 Transcranial focused ultrasound to the thalamus is associated with reduced extracellular GABA levels in rats *Neuropsychobiology* **65** 153–60

Yoo S S, Bystritsky A, Lee J H, Zhang Y, Fischer K, Min B K, McDannold N J, Pascual-Leone A and Jolesz F A 2011a Focused ultrasound modulates region-specific brain activity *Neuroimage* **56** 1267–75

Yoo S S, Kim H, Min B K, Franck E and Park S 2011b Transcranial focused ultrasound to the thalamus alters anesthesia time in rats *Neuroreport* **22** 783–7

Younan Y, Deffieux T, Larrat B, Fink M, Tanter M and Aubry J F 2013 Influence of the pressure field distribution in transcranial ultrasonic neurostimulation *Med. Phys.* **40** 082902

Young R R and Henneman E 1961 Reversible block of nerve conduction by ultrasound: ultrasonic blocking of nerve fibers *Arch. Neurology* **4** 83–9